

University of Groningen

PbS nanocrystal solar cells with high efficiency and fill factor

Szendrei, K.; Gomulya, W.; Yarema, M.; Heiss, W.; Loi, M. A.

Published in:
Applied Physics Letters

DOI:
[10.1063/1.3518067](https://doi.org/10.1063/1.3518067)

IMPORTANT NOTE: You are advised to consult the publisher's version (publisher's PDF) if you wish to cite from it. Please check the document version below.

Document Version
Publisher's PDF, also known as Version of record

Publication date:
2010

[Link to publication in University of Groningen/UMCG research database](#)

Citation for published version (APA):

Szendrei, K., Gomulya, W., Yarema, M., Heiss, W., & Loi, M. A. (2010). PbS nanocrystal solar cells with high efficiency and fill factor. *Applied Physics Letters*, 97(20), 203501-1-203501-3. [203501].
<https://doi.org/10.1063/1.3518067>

Copyright

Other than for strictly personal use, it is not permitted to download or to forward/distribute the text or part of it without the consent of the author(s) and/or copyright holder(s), unless the work is under an open content license (like Creative Commons).

The publication may also be distributed here under the terms of Article 25fa of the Dutch Copyright Act, indicated by the "Taverne" license. More information can be found on the University of Groningen website: <https://www.rug.nl/library/open-access/self-archiving-pure/taverne-amendment>.

Take-down policy

If you believe that this document breaches copyright please contact us providing details, and we will remove access to the work immediately and investigate your claim.

Downloaded from the University of Groningen/UMCG research database (Pure): <http://www.rug.nl/research/portal>. For technical reasons the number of authors shown on this cover page is limited to 10 maximum.

PbS nanocrystal solar cells with high efficiency and fill factor

K. Szendrei,¹ W. Gomulya,¹ M. Yarema,² W. Heiss,² and M. A. Loi^{1,a)}

¹Zernike Institute for Advanced Materials, University of Groningen, Nijenborgh 4, Groningen 9747 AG, The Netherlands

²Institute for Semiconductor and Solid State Physics, University of Linz, Altenbergerstr. 69, Linz 4040, Austria

(Received 22 September 2010; accepted 28 October 2010; published online 15 November 2010)

We report on the fabrication of efficient PbS solar cells, showing power conversion efficiencies approaching 4% and fill factors of 60% under AM1.5 illumination. The effect of the size of two different nanocrystals (NCs) on the performance and key parameters of the devices are discussed together with peculiar features of device functioning. The results prove that the devices are not under space-charge limitation and the device performance is influenced by charge trapping which is dependent on the size of the NCs. © 2010 American Institute of Physics. [doi:10.1063/1.3518067]

Photovoltaic devices^{1–3} and photodetectors^{4–6} based on solution-processable colloidal inorganic nanocrystals (NCs) have recently received increasing attention thanks to the unique optical and electrical properties⁷ of the NCs. Due to quantum confinement, the tunability of the band gap allows to maximize the absorption of solar radiation in the near-infrared region for narrow band gap semiconductors such as PbS and PbSe. Until now, the presence of the insulating molecular shell around the NCs was considered to be the major drawback preventing their use in electronics and optoelectronics. Recently, several methods^{8–13} have been developed to replace long insulating molecules such as oleic acid (OA) by shorter ligands which can reduce interparticle spacing and increase the electronic coupling between NCs. To fabricate optoelectronic devices, in most of these reports ethanedithiol^{14,15} or benzenedithiol^{11,12,16} (BDT) are used as bidentate ligands to exchange the original insulating ligands and crosslink the NCs after thin film deposition.

The active layer of these solar cells is generally fabricated by sequential layer by layer (LBL) deposition such as dipping¹⁵ or spin-coating^{11,16} of the NC and thiol solutions. Promising solar cells have been reported using PbS,^{14,17} PbSe,¹⁵ or PbS_xSe_{1–x} NCs¹⁸ as active layer, boosting power conversion efficiencies (PCE) up to 3.6%.¹⁶ Solar cells based on junctions between PbX NCs and other semiconductors have also been reported.^{11,19–22} In a recent report,²¹ the figures of merit of different device architectures are compared and the major limitations of NC photovoltaic devices are identified as: (i) low open-circuit voltage (V_{oc}), approximately equal to half of the band gap of the NCs, and (ii) low fill factor (FF).

In the present work, we report on the fabrication of efficient PbS solar cells, showing PCEs approaching 4% and FFs of 60% on a device active area of 4 mm². Our results exceed the previously reported literature record¹⁶ where a PCE of 3.6% and a FF of 51% were obtained on an active area of 2.9 mm². The device active layer (~140 nm) was prepared between an ITO anode and a 1 nm LiF/100 nm Al cathode by a LBL sequential spin-coating method using 5 mg/ml solutions of PbS in chloroform and 0.02M 1,4-BDT in acetonitrile. To replace the insulating OA ligands by 1,4-

BDT, in each iteration PbS was spin coated at 4000 rpm followed by soaking of the PbS layer in the 1,4-BDT solution for 30 s and spin-coating at 4000 rpm to remove residual solution. Each iteration produces 6–7 nm of PbS film which allows to precisely control the overall layer thickness.

The ligand exchange in the PbS thin film was followed by Fourier transform infrared spectroscopy (FTIR). The FTIR spectra reported in Fig. 1(a) confirm that the original insulating oleic acid ligands are replaced by the much shorter BDT in agreement with a previous report.¹² The characteristic vibrations of oleic acid [top part Fig. 1(a)] such as the strong symmetrical and asymmetrical (COO[–]) vibrations at ~1400 and 1550 cm^{–1} and the C–H vibrations at ~2856 and 2925 cm^{–1} are strongly reduced in the BDT treated film [bottom Fig. 1(a)]. In contrast, the typical vibrations of BDT such as C=C at ~1465 cm^{–1}, p-benzene at ~805 cm^{–1}, and the C–S stretch peaks at ~660 cm^{–1} appeared. The peaks at ~1093 cm^{–1} in the FTIR spectra of the BDT treated NCs layer are attributed to the Si substrate, being here more evident because of the smaller film thickness respect to the OA-NCs film. Moreover, the BDT treated sample shows a feature at 487 cm^{–1} which can be attributed to the formation of S–S bonds. The schematic illustration of PbS NCs cross-linked with BDT molecules is shown in Fig. 1(b). The topography of the layers formed by cross-linked NCs was obtained by an atomic force microscope (AFM) operating in tapping mode [Fig. 1(c)]. The surface of

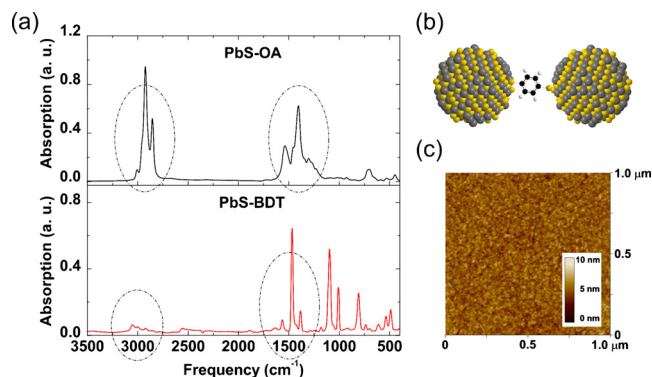


FIG. 1. (Color online) (a) FTIR spectroscopy characterization of PbS thin films before and after BDT treatment. (b) Schematic of PbS NCs cross-linked with BDT. (c) AFM topography image of BDT treated PbS thin films.

^{a)}Electronic mail: m.a.loi@rug.nl.

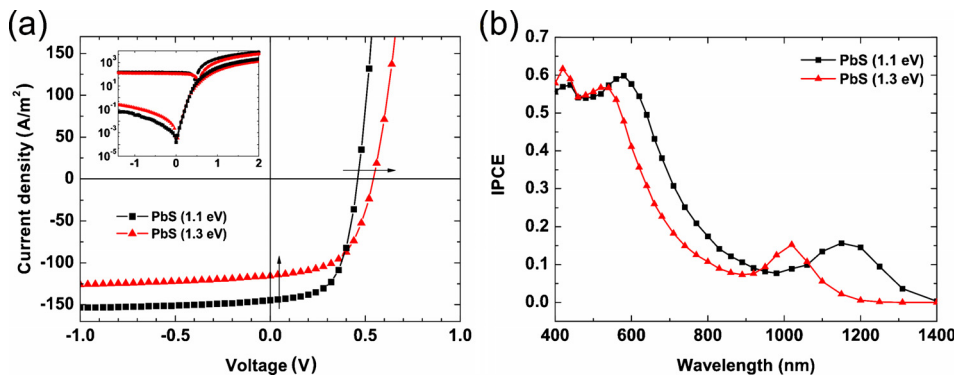


FIG. 2. (Color online) (a) J-V characteristics of PbS solar cells composed of two different types of NCs. Inset: J-V curves on a logarithmic scale in dark and under illumination. (b) IPCE spectra of PbS solar cells.

the active layer appears to be quite smooth with a rms roughness of 1.7 nm.

The current density-voltage (J-V) characteristics of the BDT treated PbS solar cells are shown in Fig. 2(a). The devices were fabricated using two different sizes of PbS NCs with diameters of 3.5 (band gap of 1.3 eV) and 4.3 nm (band gap of 1.1 eV), resulting in PCEs of 3.48% and 3.93%, respectively. Note that after 21 days of storage in N_2 the device efficiency decreased to $\sim 80\%$ of the original value. Current-voltage characteristics of these devices were measured in nitrogen atmosphere under illumination of a white light metal halide lamp calibrated by a Si reference cell. The PbS solar cells made with the smaller NCs exhibit higher V_{oc} (0.55 V instead of 0.46 V) due to the larger band gap. On the contrary, the J_{sc} of the device fabricated with the 4.3 nm PbS NCs is much larger. This higher short-circuit current could be due to the reduced band gap, resulting in more extended absorption, as shown by the IPCE measurements in Fig. 2(b), or by the reduced amount of trapping sites at the interface in the films composed of bigger NCs. The IPCE spectra were measured from 400 to 1400 nm relative to that of a calibrated Si and a Ge photodiode. For both NCs the IPCE shows a maximum of $\sim 60\%$ in the visible and $\sim 20\%$ in the infrared region. The calculated J_{sc} of the devices from the IPCE data under 100 mW/cm^2 of AM1.5G solar irradiation were 113.6 A/m^2 in the case of smaller NCs and 144.5 A/m^2 for the NCs with a band gap of 1.1 eV, showing good agreement with the J-V measurements [see Fig. 2(a)]. The devices fabricated using larger NCs show FF exceeding 60% (64% the best FF achieved), while in the case of the smaller NCs the FF is as high as 56%. This lower value of the FF could be a sign of slightly more efficient recombination of the electron-hole pairs in the active layer. Similar FFs were only presented recently by Zhao *et al.*,²³ however for bilayer hybrid devices using PbS NCs and fullerene derivatives as active

layers. The very high FF values of our devices also suggest that the photocurrent is not space-charge limited.²⁴

To further prove that our devices are not space-charge limited, we apply a simple physical model developed by Goodman and Rose for photoconductive layers.²⁵ Therefore, the variation of J_{sc} with the light intensity is plotted in double logarithmic scale in Fig. 3(a). The slopes (S) of both curves were determined from the fit to the experimental data, resulting in $S \sim 1$. This confirms that the photocurrent is not space-charge limited, but is only determined by the generation rate of photoexcitations upon illumination. It has been shown that a space-charge limited photocurrent shows a square root dependence on the effective voltage and a slope $S \sim 0.75$ due to the formation of space-charge regions.^{24,25}

Figure 3(b) shows the photocurrent $J_{ph} = J_L - J_D$, where J_L and J_D are the current density under illumination and in dark, respectively, as a function of the effective voltage ($V_0 - V$). The effective voltage was obtained by subtracting the applied voltage (V) from the compensation voltage (V_0) which is defined as $J_{ph} = 0$. In Fig. 3(b) only two regimes can be distinguished: (i) small effective voltages ($V_0 - V < 0.1 \text{ V}$) where the drift and diffusion currents compete and vary linearly with the voltage and (ii) increasing effective voltages ($V_0 - V > 0.1 \text{ V}$) when the J_{ph} tends to saturate. The third regime where the J_{ph} would be characterized by the square root of the effective voltage does not appear, confirming once more that the devices are not space-charge limited. When space-charge effects do not play any role and the recombination is neglected, the photocurrent can be expressed by $J_{ph} = qGL$ where q is the electric charge, G is the generation rate of the photoexcitations, and L is the device layer thickness.²⁵ Using the maximum J_{ph} values obtained from the saturation regime of the plots, the generation rates G_{max} were calculated to be $7 \times 10^{27} \text{ m}^{-3} \text{ s}^{-1}$ (for NCs of 1.1 eV) and 5.4

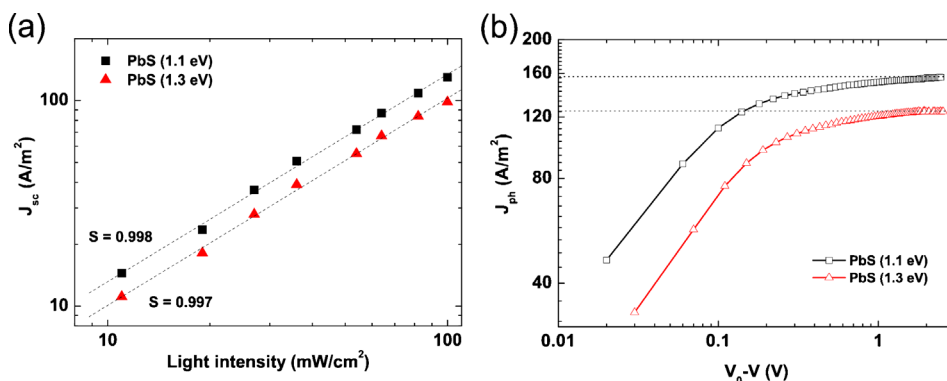


FIG. 3. (Color online) (a) Light intensity dependence of the short-circuit current (J_{sc}) and (b) photocurrent (J_{ph}) of the PbS devices vs. the effective applied voltage ($V_0 - V$).

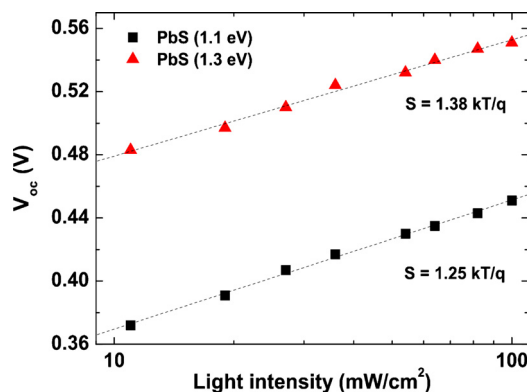


FIG. 4. (Color online) Open-circuit voltage (V_{oc}) vs the natural logarithmic of the light intensity of PbS solar cells.

$\times 10^{27} \text{ m}^{-3} \text{ s}^{-1}$ (for NCs of 1.3 eV). Clearly, the devices composed of larger NCs absorb more light which leads to the generation of more photoexcitations.

The device active layer can be treated as one intrinsic semiconducting material with relatively low mobility,^{13,23} which can be described by the metal-insulator-metal model. To further understand the working mechanism and limiting factors of these solar cells, the V_{oc} of the two different NC devices were plotted versus the logarithm of the light intensity (Fig 4). For trap-free solar cells, the slope (S) of the V_{oc} should follow $S = (kT/q)$, where k is the Boltzmann constant, T is the temperature, and q is the elementary charge.^{26,27} However, it has been demonstrated that trap-assisted recombination could enhance the dependence of the V_{oc} on the light intensity.²⁸ For our devices, the slopes were calculated from the linear fits, resulting in $S = 1.38 \text{ (kT/q)}$ for smaller NCs and $S = 1.25 \text{ (kT/q)}$ for the bigger NCs, indicating the presence of traps in the active layers. We suggest that the difference between the two devices originates from the depth lowering of the traps and a decrease of the amount of interfaces in the active layer when increasing the size of the NCs. These results support the idea of a recent report where the performance of PbSe devices are considered to improve by changing the depth of trap states with NC band gap.²⁹

In summary, we fabricated solar cells using PbS NCs of two different diameters. The devices show excellent characteristics, exceeding the former best reports with PCE of 3.93% and FF of 60% under AM1.5 illumination. We demonstrated that the J_{sc} of the solar cells depend linearly on the light intensity and no space-charge effects occur. Moreover, we showed that the active layers are affected by trapping. A further improvement in the NC layer fabrication limiting the charge trapping could lead to highly efficient solar cells.

Financial support from the European Commission through the Human Potential Programs (RTN Nanomatch, Contract No. MRTN-CT-2006-035884) and from the Austrian Science Fund FWF (Project SFB-IRON) is gratefully acknowledged. The authors thank K. U. Loos and E. J.

Vorenkamp for the FTIR measurements and F. van der Horst and J. Harkema for technical support. K.Sz. thanks P. de Bruyn, M. Kuik, and G. A. H. Wetzelaer for fruitful discussions.

- ¹A. J. Nozik, *Physica E (Amsterdam)* **14**, 115 (2002).
- ²E. H. Sargent, *Adv. Mater. (Weinheim, Ger.)* **20**, 3958 (2008).
- ³H. W. Hillhouse and M. C. Beard, *Curr. Opin. Colloid Interface Sci.* **14**, 245 (2009).
- ⁴S. A. McDonald, G. Konstantatos, S. Zhang, P. W. Cyr, E. J. D. Klem, L. Levina, and E. H. Sargent, *Nature Mater.* **4**, 138 (2005).
- ⁵T. Rauch, M. Boberl, S. F. Tedde, J. Furst, M. V. Kovalenko, G. Hesser, U. Lemmer, W. Heiss, and O. Hayden, *Nat. Photonics* **3**, 332 (2009).
- ⁶K. Szendrei, F. Cordella, M. V. Kovalenko, M. Böberl, G. Hesser, M. Yarema, D. Jarzab, O. V. Mikhnenko, A. Gocalinska, M. Saba, F. Quochi, A. Mura, G. Bongiovanni, P. W. M. Blom, W. Heiss, and M. A. Loi, *Adv. Mater. (Weinheim, Ger.)* **21**, 683 (2009).
- ⁷A. P. Alivisatos, *J. Phys. Chem.* **100**, 13226 (1996).
- ⁸D. V. Talapin and C. B. Murray, *Science* **310**, 86 (2005).
- ⁹M. Law, J. M. Luther, Q. Song, B. K. Hughes, C. L. Perkins, and A. J. Nozik, *J. Am. Chem. Soc.* **130**, 5974 (2008).
- ¹⁰D. A. R. Barkhouse, A. G. Pattantyus-Abraham, L. Levina, and E. H. Sargent, *ACS Nano* **2**, 2356 (2008).
- ¹¹S. W. Tsang, H. Fu, R. Wang, J. Lu, K. Yu, and Y. Tao, *Appl. Phys. Lett.* **95**, 183505 (2009).
- ¹²J. J. Choi, J. Luria, B. Hyun, A. C. Bartnik, L. Sun, Y. Lim, J. A. Marohn, F. W. Wise, and T. Hanrath, *Nano Lett.* **10**, 1805 (2010).
- ¹³E. J. D. Klem, H. Shukla, S. Hinds, D. D. MacNeil, L. Levina, and E. H. Sargent, *Appl. Phys. Lett.* **92**, 212105 (2008).
- ¹⁴J. Tang, X. Wang, L. Brzozowski, D. A. R. Barkhouse, R. Debnath, L. Levina, and E. H. Sargent, *Adv. Mater. (Weinheim, Ger.)* **22**, 1398 (2010).
- ¹⁵J. M. Luther, M. Law, M. C. Beard, Q. Song, M. O. Reese, R. J. Ellingson, and A. J. Nozik, *Nano Lett.* **8**, 3488 (2008).
- ¹⁶R. Debnath, J. Tang, D. A. Barkhouse, X. Wang, A. G. Pattantyus-Abraham, L. Brzozowski, L. Levina, and E. H. Sargent, *J. Am. Chem. Soc.* **132**, 5952 (2010).
- ¹⁷J. Tang, L. Brzozowski, D. A. R. Barkhouse, X. Wang, R. Debnath, R. Wolowiec, E. Palmiano, L. Levina, A. G. Pattantyus-Abraham, D. Jankosmanovic, and E. H. Sargent, *ACS Nano* **4**, 869 (2010).
- ¹⁸W. Ma, J. M. Luther, H. Zheng, Y. Wu, and A. P. Alivisatos, *Nano Lett.* **9**, 1699 (2009).
- ¹⁹J. J. Choi, Y. Lim, M. B. Santiago-Berrios, M. Oh, B. Hyun, L. Sun, A. C. Bartnik, A. Goedhart, G. G. Malliaras, H. D. Abruña, F. W. Wise, and T. Hanrath, *Nano Lett.* **9**, 3749 (2009).
- ²⁰K. S. Leschkes, T. J. Beatty, M. S. Kang, D. J. Norris, and E. S. Aydil, *ACS Nano* **3**, 3638 (2009).
- ²¹A. G. Pattantyus-Abraham, I. J. Kramer, A. R. Barkhouse, X. Wang, G. Konstantatos, R. Debnath, L. Levina, I. Raabe, M. K. Nazeeruddin, M. Grätzel, and E. H. Sargent, *ACS Nano* **4**, 3374 (2010).
- ²²S. Tsang, H. Fu, J. Ouyang, Y. Zhang, K. Yu, J. Lu, and Y. Tao, *Appl. Phys. Lett.* **96**, 243104 (2010).
- ²³N. Zhao, T. P. Osedach, L. Chang, S. M. Geyer, D. Wanger, M. T. Binda, A. C. Arango, M. G. Bawendi, and V. Bulovic, *ACS Nano* **4**, 3743 (2010).
- ²⁴V. D. Mihailetschi, J. Wildeman, and P. W. M. Blom, *Phys. Rev. Lett.* **94**, 126602 (2005).
- ²⁵A. M. Goodman, *J. Appl. Phys.* **42**, 2823 (1971).
- ²⁶S. Sze and K. K. Ng, *Physics of Semiconductor Devices* (Wiley, Hoboken, NJ, 2006).
- ²⁷L. J. A. Koster, V. D. Mihailetschi, R. Ramaker, and P. W. M. Blom, *Appl. Phys. Lett.* **86**, 123509 (2005).
- ²⁸M. M. Mandoc, F. B. Kooistra, J. C. Hummelen, B. de Boer, and P. W. M. Blom, *Appl. Phys. Lett.* **91**, 263505 (2007).
- ²⁹Y. Liu, M. Gibbs, J. Puthussery, S. Gaik, R. Ihly, H. W. Hillhouse, and M. Law, *Nano Lett.* **10**, 1960 (2010).